Chemical Physics 413 (2013) 89–101

Contents lists available at SciVerse ScienceDirect

Chemical Physics

journal homepage: www.elsevier.com/locate/chemphys

Electronic structure and optical spectra of semiconducting carbon nanotubes functionalized by diazonium salts

Jessica Ramirez [a], Michael L. Mayo [c], Svetlana Kilina [c,*], Sergei Tretiak [b]

[a] Quantum Theory Project, Departments of Chemistry and Physics, University of Florida, Gainesville, FL 32611, USA
[b] Theoretical Division, Center for Nonlinear Studies (CNLS), and Center for Integrated Nanotechnologies (CINT), Los Alamos National Laboratory, Los Alamos, NM 87545, USA
[c] Department of Chemistry and Biochemistry, North Dakota State University, Fargo, ND 58108, USA

ARTICLE INFO

Article history:
Received 29 May 2012
In final form 18 October 2012
Available online 7 November 2012

Keywords:
Carbon nanotubes
Exciton brightening
Aryl diazonium reagents
Density functional theory
Chemical functionalization

ABSTRACT

We report density functional (DFT) calculations on finite-length semiconducting carbon nanotubes covalently and non-covalently functionalized by aryl diazonium moieties and their chlorinated derivatives. For these systems, we investigate (i) an accuracy of different functionals and basis sets, (ii) a solvent effect, and (iii) the impact of the chemical functionalization on optical properties of nanotubes. In contrast to B3LYP, only long-range-corrected functionals, such as CAM-B3LYP and wB97XD, properly describe the ground and excited state properties of physisorbed molecules. We found that physisorbed cation insignificantly perturbs the optical spectra of nanotubes. In contrast, covalently bound complexes demonstrate strong redshifts and brightening of the lowest exciton that is optically dark in pristine nanotubes. However, the energy and oscillator strength of the lowest state are dictated by the position of the molecule on the nanotube. Thus, if controllable and selective chemical functionalization is realized, the PL of nanotubes could be improved.

1. Introduction

Since first observed experimentally, by Iijima and colleagues [1], single walled carbon nanotubes (SWNTs) have continued to capture interest from a variety of fields related to science, technology, and industry – in large part, on the basis of their one-of-a-kind chemical, spectroscopic, mechanical, and structural features. The 'tunability' and stability of the optical and electronic properties of SWNTs have given them promise as advanced materials capable of use in modern devices, such as highly sensitive chemical sensors [2,3], field effect transistors [4,5], quasi-1D quantum wires [6], and as adjustable components in optoelectronic instrumentation [7–9]. In these applications, the structural aspects of carbon nanotubes – in particular, the nanotube diameter and chirality – modulate their chemical and electronic behaviors and thus control the overall performance of a SWNT-based device. However, methods of cost-efficient and reliable identification and separation of nanotubes on the basis of their identical diameter, chirality, and electronic type from inhomogeneous SWNTs mixtures are still not well developed impeding the practical incorporation of nanotubes into the design of upcoming technologies [10]. This challenge has motivated various studies on the incorporation of subsidiary functional molecules into raw nanotube solutions. Covalent [11–13] and non-covalent [14–16] chemical functionalization of nanotubes suggests one of the simplest methods for tube separation by manipulating the intrinsic properties of as-synthesized nanotubes samples. In addition, many desirable qualities, including tube solubility and unbundling, can also be improved via SWNT chemical functionalization.

Water-soluble aryl diazonium salts have demonstrated success as reagents to achieve arylation of aromatic compounds [17,18] – thereby inspiring the utilization of their chemistry for developing a post-synthesis approach for the selective separation of heterogeneous nanotube mixtures [19,20]. One of the possible scenarios of such a reaction suggests that the aryl ring forms a covalent bond with a nanotube surface in a two-step pathway: first, the diazonium cation adsorbs quickly (and noncovalently) to the outer tube surface (about 2.4 min) [21]. The π–π character of tube-cation interaction allows for the electron transfer from the tube to the diazonium molecule forming a charge-transfer transition complex. The complex then decomposes at a slow rate-limiting step (about 73 min) into N_2 gas and aryl radical, forming a mixture of covalently and noncovalently bound products, where the large majority of the sample population is attributed to the covalent nanotube-aryl interaction [21]. The selectivity of this process is reflected in the preferential reaction of metallic over semiconducting tubes [22,23]. However, it is known that aryl diazonium salts have very complicated chemistry in solution due to the variety of reaction pathways with a large number of potential intermediates and products. Therefore, the exact pathway of aryl diazonium reactions

* Corresponding author.
E-mail address: svetlana.kilina@ndsu.edu (S. Kilina).

0301-0104/$ - see front matter © 2012 Elsevier B.V. All rights reserved.
http://dx.doi.org/10.1016/j.chemphys.2012.10.010

with SWNTs is still under debate and different mechanisms of reaction have been suggested [23,21,24,25]. In addition, recent studies have revealed the dominant role of surfactants in the selectivity of semiconducting vs. metallic SWNT-aryl diazonium systems and suggest a strong dependence on the choice of surfactant in the reaction between SWNT and aryl diazonium, where the surfactant acts synergistically with a solvent to electrostatically attract, exclude, or chemically modify the diazonium complex [26,27].

Because of various pathways of possible reactions between the SWNT, aryl diazonium salt, and their solvent environment, as well as the extended size of the system (more than 1000 atoms in a SWNT), computational simulations of these reactions are very challenging. Therefore, a limited number of computational efforts have been done in studying SWNT-aryl diazonium systems [28,29,27,30] and related compounds [31,32], with the main focus on the morphology and packing of salt molecules at the nanotube surface utilizing classical molecular dynamics (MD) [27,30,31]. First principle calculations based on density functional theory (DFT) have been conducted for the smallest armchair and zigzag nanotubes interacting with aryl diazonium cation. These calculations have shown that the electronic properties of the aryl diazonium-nanotube system changes upon formation of both the physisorbed and chemisorbed adsorbate-substrate complexes [28] leading to hybridized adsorbate-SWNT molecular orbitals. Such orbitals have stronger hybridized character in the case of metallic nanotubes and are expected to facilitate electron transfer from a nanotube to the aryl diazonium adsorbent needed for aryl chemisorption to the nanotube surface, which could explain the selectively of the reaction with metallic SWNTs. However, the level of orbital delocalization strongly depends on the DFT functional; therefor, the above conclusion might be questionable if the effect of methodology is not systematically analyzed. Recently, the reaction pathways have been simulated based on two-layer ONIOM methodology [29] treating aryl diazonium with DFT utilizing the B3LYP functional and 6-31G* basis set, while the SWNT is calculated at the semiempirical AM1 level of theory. The simulations confirmed that the reaction between the (5,5) SWNT and aryl diazonium derivatives occurs in a two-step process: a surface chemical adsorption followed by a covalent bonding, where the covalent reaction controls the overall rate of reaction.

However, reaction energies, activation barriers, binding energies, the energy alignment of electronic orbitals, and their delocalization properties are sensitive to the DFT methodology used for calculations [33]. To ensure the validity of results, the correct combination of DFT functional and basis set must be used to derive an appropriate Kohn–Sham wavefunction, since it includes all electronic and spatial information describing the system. Such analysis is especially important for the physisorption case, since commonly used functionals (e.g., hybrid exchange-correlation functionals such as B3LYP) typically fail in predictions of weak dispersion interactions. Nonetheless, systematic analysis and comparisons of the computational methods – in particular, differences in the performance of the hybrid exchange-correlation functionals [34] vs. the new generation of asymptotically-corrected functionals [33,35] recently developed for better description of long-range electronic communication and Van der Waals types of interactions – have not been carried out for investigations of nanotube-aryl diazonium salts interactions, their electronic structures, and optical spectra. Thus, concurrent with the advent of a new class of DFT models, is the growing importance to understand how results from computational investigations are affected by differences in methodological choices, e.g., implementation of various functionals, basis sets, and solvent effects. In addition, no theoretical investigations of the effect of the covalent and non-covalent functionalization of nanotubes by diazonium salts on their optical properties have been reported so far, while insights on this question can help to better understand nanotube-diazonim interaction mechanisms.

In this article, we use both hybrid (B3LYP) and long-range-corrected (CAM-B3LYP [36] and wB97XD [35]) exchange-correlation kernels to study chiral semiconductor (6,2), (6,5) and zigzag (8,0) SWNTs covalently and non-covalently functionalized by aryl diazonium moieties, elucidating the spatial and electronic structures of the major reactant and products of this reaction [21,29]. Our main interest is to assess the sensitivity of DFT calculations on the computational method that is used for studying the ground and excited state properties of such highly conjugated systems. Specifically, we examine how the inclusion of long-range corrections and empirical dispersions to the density functional affects the modeling of SWNT-aryl diazonium cation interactions, the ground state geometries, electronic band structures, and localization/delocalization properties of molecular orbitals. As expected, the long-range-corrected functionals provide more appropriate descriptions of the π–π interactions between the nanotube and molecule than the B3LYP functional.

We also investigate the role of long-range interactions on the excited state properties and optical spectra using time-dependent DFT (TD–DFT) approach in vacuum and effective solvent media. Applying the appropriate TD–DFT methodology, we study the effect of the covalent and noncovalent functionalization of the SWNTs by diazonium salts on the optical properties of nanotubes. Calculated absorption spectra indicate that covalent attachment of the aryl ring to the SWNT leads to a pronounced red shifting and brightening of the formerly dark first exciton of the SWNT. This finding contradicts a common assumption that chemical defects should always depress the SWNT emission due to formation of optically forbidden trap states. Nonetheless, our results agree well with recent investigations on the effect of hydrogenation of SWNT surfaces [37,38] that demonstrate the rising intensity of satellite peaks at the lower-energy end of the PL spectra upon adsorption of atomic hydrogen onto the SWNT surface.

2. Methodology and computational details

2.1. Ground state computations

We focus on three narrow diameter (<1 nm) semiconducting nanotubes (6,2), (6,5), and (8,0) with a non-covalently adsorbed aryl diazonium cation (initial reactants of the reaction [21,29]) and with a covalently adsorbed aryl radical (the final product of the reaction [21,29]). The latter perturbs locally the π-conjugation of the SWNT by introducing a partial sp^3 bonding character for the respective nanotube carbons bound to the aryl ring, while the other carbon, of the same carbon-ring of the nanotube, is saturated by a hydrogen creating the 'para'-defect at the SWNT side-wall (see Fig. 2). Additional calculations of the doubly arylated (6,2) and (6,5) SWNTs have been also performed. These hybrid structures were prepared from initially optimized by wB97XD/3-21G* arly-SWCNT geometries by removing the attached hydrogen atom and mirroring the functionalization circumferentially by adding the second aryl substituent to the opposite side of the tube. In this way, two sp^3 defects are introduced at the mid-tube position at *different* carbon-rings as far apart as possible. We have also considered the chlorinated derivatives of these systems, which were obtained by substitution of the para-hydrogens (on the two attached aryl groups) with chlorine atoms. On average, the aryl-SWNT bond distance was 1.555 Å and the C–Cl bond (on the aryl group) was 1.750 Å.

The nanotubes studied were constructed as finite segments consisting of several lattice units of a similar approximate length

ranging from about 21 to 38 Å. To ensure that the natural symmetry of the tubes is retained, an integral number of unit cells were used to construct each model: two, one, and six units for the (6,2), (6,5) and (8,0) tubes, respectively. Hydrogen atoms were used to saturate all dangling bonds left open at the tube ends, capping the SWNT to prevent the appearance of mid-gap states (as described in detail in Ref. [39]). With regard to the finite sized SWNTs used in this study, the effects of the nanotube size on optical properties of SWNTs has been addressed in numerous studies [39–42]. It was shown that models of capped, short finite sized SWNTs such as those used in this study, are well suited to qualitatively reproduce photophysical properties in the infinite length limit.

The Becke 3-parameter hybrid functional (B3LYP) [43,44], having a 20% fraction of Hartree–Fock (HF) exchange, is one of the most widely used DFT exchange-correlation kernels for modeling the electronic and optical properties of large organic molecules [45]. In situations where accurate treatment of the non-locality of the exchange-correlation hole is essential, B3LYP and other semi-local correlation functionals fail to capture long-range dynamical correlation effects [35,46,47]. We have assessed B3LYP as well as the recently developed asymptotically corrected wB97XD functional of Chai and Head-Gordon [35], which has a 100% fraction of the HF exchange at long-range and about 22% at short-range, as well as incorporates empirical dispersion corrections.

To evaluate the influence of the basis set size on the results of our DFT simulations, geometry optimizations were performed using the STO-3G minimal basis of Slater-Type orbitals [48], and Pople 3-21G split-valence basis of Gaussian-Type orbitals [49]. The DFT/3-21G level of theory has been advocated as sufficient for attaining geometries of the diazonium-nanotube systems and their electronic structures [28], as well as the optical properties of pristine SWNTs [42,39,37]. To verify the validity of this assertion with respect to our results, calculations were also performed using a 6-31G*/3-21G mixed basis, with the larger 6-31G* basis set having its basis functions centered on the atoms of aryl diazonium and a few atoms of the SWNT in the vicinity of the location of adsorption site, while the 3-21G basis set was used for all other atoms. Utilization of such mixed basis sets is reasoned by the significant size of the systems we study (about 400 atoms), which severely limits applications of extended basis sets. There is a trade-off inherent in our computational studies between the complexity/size of the systems studied and the theoretical accuracy that may be achieved. Here, we chose to perform highly intensive DFT calculations utilizing relatively large basis sets (involving multiple orbitals centers per atom) and long-range-corrected functionals for systems having of 400 atoms (~4 nm in length). Due to high computational expanse, we were limited to smaller systems; however, at the advantage of being able to implement more advanced level of theory than those is typically used for extended systems.

Using the above mentioned different functional/basis combinations, the DFT geometry optimizations of all systems were performed utilizing the GAUSSIAN09 [50] software package, until an energy convergence limit of 10^{-6} Hartrees was reached. Based on the DFT optimization results, the binding energies between the aryl diazonium and SWNT were calculated according to the standard definition: Energies of individually optimized components (isolated aryl diazonium cation and isolated SWNT) were subtracted from the total energy of the optimized SWNT-aryl diazonium hybrid structure. Solvent effects were further included via embedding the molecule in a polarizable continuum medium with an appropriate dielectric constant in the framework of the conductor-like polarizable continuum model (CPCM) [51,52], as implemented in the GAUSSIAN09 code. Acetonitrile ($\epsilon = 35.688$) has been chosen as a common example of a polar solvent to explore the solvent media effects on the SWNT-aryl diazonium interaction.

2.2. Excited state calculations

Subsequent excited-state calculations were carried out using a linear response adiabatic TD–DFT approach, as implemented in the GAUSSIAN09 package. Geometries optimized at the wB97XD/3-21G level of theory were used as an input for all TD–DFT calculations, both for the physisorbed cation and the covalently attached aryl radical due to the higher accuracy of the obtained structures. It was shown before that hybrid DFT models (including a fraction of orbital exchange into the kernel) allow for an accurate description of bound excitonic states in conjugated organic materials [53–55] and, in particular, carbon nanotubes [42,56,57]. Therefore, we have used the B3LYP functional for the majority of our calculations. However, within the framework of TD–DFT, conventional exchange-correlation functionals with a small fraction of orbital exchange have been shown to fail for calculations of excitations in many compounds introducing spurious charge-transfer (CT) character, especially in the asymptotic regions of molecular systems [58,59,45,60,61].

To check that these artificial CT states are not present in the B3LYP results, especially in the case of non-covalently functionalized nanotubes, excited states were also calculated using the long-range-corrected functionals such as wB97XD [35] and CAM-B3LYP [36]. The latter is based on a Coulomb-attenuating method comprised of 19% HF exchange interaction at the short-range and 65% at the long-range. The 3-21G basis set was used in all TD–DFT calculations. The 20 lowest excited-state transition energies and their respective oscillator strengths were computed for each molecular system. The absorption spectra were further simulated using a Gaussian line shape with an empirical line-broadening parameter of 10 and 50 meV to mimic various broadening effects occurring under experimental conditions.

3. Results and discussions

3.1. Structural aspects: SWNT–aryl interactions

Aryl diazonium cation physisorbed on the SWNT surface. Previous studies [62,63] have shown that an impurity or a trap state induced during chemical bonding are characterized by a relatively delocalized wavefunction, while the physisorbed molecules usually have a localized character of orbitals. The degree to which the molecular orbitals of two separate compounds undergo hybridization is dependent on the strength and nature of the interaction they share. In Fig. 1, the charge-density surfaces of the highest occupied (HOMO) and lowest unoccupied (LUMO) molecular orbitals, associated with the optimized geometries of the aryl diazonium cation $C_6H_5N_2^+$ adsorbed on the (6,2) nanotube, reveal stark differences in orbital hybridization for different methodologies used. According to the B3LYP/STO-3G calculation (Fig. 1(a)), the favored orientation of the diazonium cation on the SWNT is nearly parallel with respect to the tube surface, while the aryl ring is significantly tilted with respect to the N_2^+ group. This alignment seems to signify the presence of forces between the two interacting systems, induced by the predisposition of the π-orbitals of each compound to establish π–π overlap between the aryl substituent and the nanotube wall. The prevalence of this strong hybridization, most apparent in the LUMO, is reminiscent of covalent bonding and is in good agreement with previous DFT calculations [28]. Yet, we assume this is a false artifact due to the truncated STO-3G basis set, since the minimal STO-3G basis set is known to poorly describe the tails of atomic orbital functions, leading to erroneous structural predictions and artificial π–π interactions [33].

As shown in Fig. 1(b), progression to the B3LYP/3-21G level of theory leads to the adoption of a more perpendicular orientation

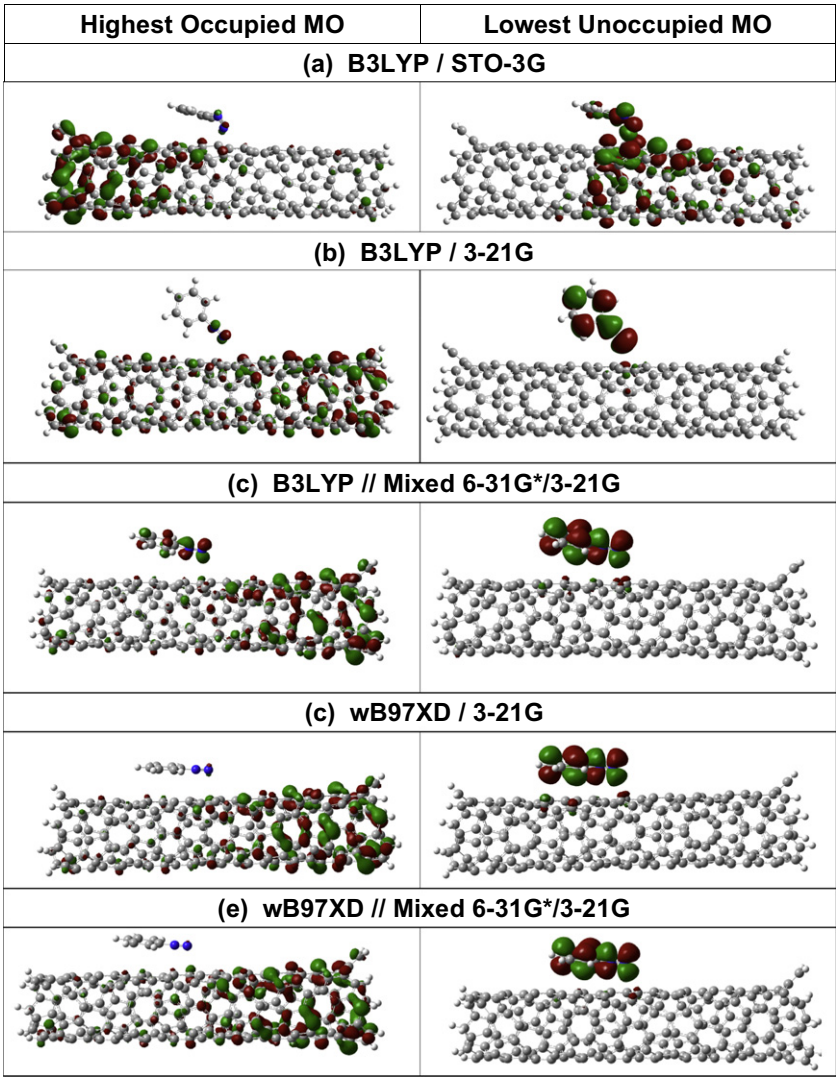

Fig. 1. Comparison of the highest-occupied (left) and lowest-unoccupied (right) molecular orbitals associated with the physisorbed $C_6H_5N_2^+$–(6,2) systems, as calculated with different DFT methodologies. The red and green coloring of orbitals lobes depicts the alternating spatial extent of +/− phases of the electronic wavefunctions. (For interpretation of the references to colour in this figure legend, the reader is referred to the web version of this article.)

by the diazonium cation relative to the nanotube surface, as well as an overall increase in separation between the adsorbed molecule and the SWNT (see Table 1). Within the B3LYP/3-21G framework, the aryl group shifts further away from the tube surface, flattening the diazonium complex into a linear form with respect to the N_2^+ group, while the aryl ring is normally oriented to the SWNT surface. Such geometry indicates the absence of π–π interactions between the aryl diazonium and nanotube structures. In contrast to the highly delocalized LUMO spread over both nanotube and aryl ring as predicted by the B3LYP/STO-3G approach, the LUMO generated with the larger basis set exhibits a much smaller degree of orbital hybridization – consistent with our expectation of a non-covalent complexation as the dominant intermolecular interaction. In contrast, the HOMO exhibits some hybridization, compared to those obtained by B3LYP/STO-3G, pointing to noticeable SWNT-aryl diazonium interactions via dipole-dipole and/or charge-dipole interactions, as evidenced by the changes of the Mulliken charge on the functionalized nanotube (see the last column in Table 1).

To further study the effects of the basis set size on the nanotube-aryl diazonium interactions, we have applied a mixed basis set (see Section 2.1). Incorporation of a large mixed 6-31G*/3-21G basis set within the B3LYP functional results in a planar aryl diazonium structure with the cation approaching a distance of ~3.0–3.7 Å from the nanotube wall and oriented nearly parallel to the SWNT surface. Compared to calculations based on 3-21G basis sets, orbital delocalization is slightly increased, while still having less hybridized character than in the case of minimal STO-3G basis set, see Fig. 1(c). The molecule alignment and SWNT-aryl distances obtained with B3LYP/mixed 6-31G*/3-21G are close to typical distances in the cases of π–π interactions between two conjugated molecules, providing evidence that extended basis sets beyond 3-21G are needed for obtaining reasonable physisorbed geometries.

Due to long-range corrections, the wB97XD functional is equipped to capture dispersion effects neglected in the traditional B3LYP treatment. Fig. 1d shows that the adsorbed molecule assumes a completely parallel orientation with respect to the nanotube surface, maintaining the planarity between N_2^+ group and the aromatic aryl ring, while nanotube-aryl distances are between 3.0–3.3 Å, pointing to the π–π interactions between the nanotube and aryl diazonium. Analysis with the wB97XD/3-21G framework results in an absence of any large degree of MO hybridization between the diazonium and nanotube, consistent with the notion that electron correlations stabilize delocalized electronic

Table 1
Ground-state structural and energetic parameters for the physisorbed aryl diazonium cation on the SWNT, calculated with different DFT methodologies (functional/basis set) in vacuum: the distances between atoms of diazo-adsorbate and the nearest carbon atom of the nanotube; the angle of the adsorbate formed between two diazo nitrogens and the adjacent carbon atom of the aryl group; the energy-gap of the complexed diazonium-SWNT structure; the energy-gap of the pristine SWNT (for comparison); the binding energy of the adsorbate on the SWNT and the BSSE-corrected binding energy (appearing in parenthesis); and, the sum of Mulliken charges only on SWNT atoms.

$C_6H_5N_2^+$/*SWNT* complex	N-SWNT distance [Å]	Aryl-SWNT distance [Å]	Diazo-Aryl angle [°]	Energy gap of complex [eV]	Energy Gap of pristine SWNT [eV]	Binding energy [eV]	Mulliken charge on SWNT
B3LYP/STO-3G:							
(6,2)	1.748	3.473	127.416	0.80	2.00	−1.87 (−1.54)	0.88
(6,5)	1.836	3.805	131.689	0.62	1.83	−1.61 (−1.33)	0.85
(8,0)	1.783	3.389	129.749	0.89	2.10	−1.63 (−1.32)	0.85
B3LYP/3-21G:							
(6,2)	2.486	3.567	174.543	0.47	1.80	−0.97 (−0.76)	0.32
(6,5)	2.680	3.527	176.596	0.34	1.70	−0.99 (−0.80)	0.35
(8,0)	2.521	3.561	172.502	0.60	2.02	−0.96 (−0.76)	0.31
B3LYP/Mixed basis (3-21G and 6-31G):*							
(6,2)	3.005	3.749	176.335	0.48	1.80	−0.56	0.34
wB97XD/3-21G:							
(6,2)	2.916	3.110	178.066	2.93	4.26	−1.34 (−1.07)	0.14
(6,5)	3.059	3.227	177.427	2.55	3.81	−1.37 (−1.12)	0.12
(8,0)	3.147	3.166	177.375	2.85	4.52	−1.27 (−1.03)	0.07
wB97XD/3-21G (in solvent):							
(6,2)	3.107	3.226	179.751	4.13	4.25	−0.53	0.02
(6,5)	3.214	3.362	179.758	3.79	3.79	−0.55	0.02
(8,0)	3.354	3.248	179.150	4.35	4.53	−0.57	0.01
wB97XD/Mixed basis (3-21G and 6-31G):*							
(6,2) tube	3.005	3.309	176.538	2.87	4.27	−0.97	0.12

structures as compared to the localized ones [64]. The geometries resulting from this DFT model most closely fit expectations that the diazonium group would shift such to maximize the intermolecular forces acting between itself and the carbon nanotube to increase the π–π orbital overlaps. Extending the basis set to the mixed 6-31G*/3-21G combination has a small effect on the optimized geometries and on the orbital delocalization, as can be seen in Fig. 1(e), revealing that use of the wB97XD functional produces consistent results across several basis sets. This is in contrast to what we observe for the geometry optimization at the B3LYP level.

Note that a shift in charge density of the HOMO toward one of the edges of the nanotube (Fig. 1, the left column) calculated by wB97XD or by B3LYP with extended basis set can be explained by distortions in the nanotube orbital due to the presence of the diazonium ion – in particular, its position relative to the nanotube surface. Because the molecule is not exactly symmetrically placed with respect to the nanotube edges, the diazonium-SWNT interaction leads to a distortion of the nanotube orbital resulting in stronger delocalization on one part of the tube and less on the other. Indeed, the edges are involved, because the considered nanotubes are short. However, these distortions are expected to insignificantly affect the strength of the diazonium-SWNT interactions, since such orbitals have predominantly nanotube character with insignificant contribution from the diazonium, when appropriate functionals with long-range and dispersion corrections are used. The fact that the size of the considered nanotube is in an order of magnitude larger than the size of the diazonium molecule (4 nm vs. 0.3 nm) also can be used as an additional argument for insignificant influence of the qualitative results on diazonium-SWNT interactions by a short length of SWNTs. Thus by placing the molecule at the central part of the nanotube, it is reasonable to expect that the edge effects should be substantially eliminated. This is evidenced in Fig. 1 (right column) by the LUMO being strongly localized on the molecule with some insignificant delocalization over the central part of the nanotube. If the molecule 'feels' the nanotube edges, this orbital would have a significant portion of its charge density of the LUMO toward one of the nanotube ends, which is not observed.

Information on geometries and binding energies calculated for all functionalized nanotube systems are summarized for the non-covalent adsorption (physisorption) of $C_6H_5N_2^+$ in Table 1. It is well known that intermolecular binding energies calculated for physisorbed systems could be underestimated by hybrid functionals [65,33], owing to their failure to accurately describe the attractive London forces. This is supported by the binding energies we have calculated, as shown in Table 1. With the same basis set, the wB97XD model predicts binding energies of about 0.4 eV larger than those obtained by B3LYP calculations. Independent of the functional used, however, SWNT-aryl diazonium binding energies obtained with smaller basis sets are overestimated, with the minimal basis set resulting in a chemical binding of the $C_6H_5N_2^+$ cation to the nanotube surface. Similar decreases in the binding strength with extension of the basis set size, have been found for inorganic nanocrystalls interacting with organic ligands [66]. These trends partially originate from errors imparted by the use of a truncated set of basis functions and the basis set superposition error (BSSE), which are the most pronounced for smaller basis sets. The counterpoise correction (CP) [67] adjusts these errors and further decreases the absolute value of binding energies by 0.2–0.3 eV, as presented in Table 1.

While the effect of optimizing structures in solvent proved negligible to resulting geometries, the polar solvent has been found to have very significant effects on the SWNT-$C_6H_5N_2^+$ binding energies. Incorporation of the acetonitrile solvent environment into our calculations results in about twice smaller nanotube-aryl diazonium interactions compared to the respective gas-phase values (see Table 1). This result is not surprising, since the polar solvent should screen the nanotube-cation interactions. Note that obtained SWNT-$C_6H_5N_2^+$ binding energies (Table 1) are higher than the typical π–π interaction in a benzene dimer – 2.4 kcal/mol ($\sim$0.11 eV) in the gas phase – as calculated by the coupled cluster theory (CCSD) [68]. This difference likely originates from additional electrostatic forces between the cation and the nanotube, complementing weak π–π interactions between the aryl and SWNT surface. In fact, Mulliken charges calculated for the interacting SWNT-aryl diazonium system show small positive values at the

SWNT fragment, which indicates that some portion of electronic charge density has been transferred from the nanotube to the aryl diazonium cation. Thus, despite an absence of direct chemical bonding, the cation is stabilized through formation of the charge-transfer SWNT-aryl diazonium complex, which agrees with the suggested reaction's scenario from experimental investigations [21–23]. Polar solvent dramatically decreases this charge transfer leading to insignificant positive charge at the nanotube fragment when the complex is calculated in the presence of acetonitrile media (see Table 1). Such strong solvent effects on the electronic charge density distribution for the functionalized SWNT system confirms the important role that solvent environments play during the reaction between SWNT and aryl diazonium – controlling the charge transfer between the nanotube and aryl diazonium cation, as has been experimentally determined for these systems in the presence of different surfactants [26,27].

Past research has generated discussion regarding the spin multiplicity of the ground-state aryl diazonium cation [69,70] especially in the context of the mechanism of the analogous Meerwein reaction [71]. We performed similar calculations using the unrestricted DFT formalism for both singlet and triplet ground-states. Evaluation of these results revealed that the singlet state electronic structure calculated with unrestricted DFT is essentially the same as that obtained at the closed-shell level. The overall total energy of the triplet state was marginally higher than that obtained for the singlet system, so we focus on the singlet ground-state for subsequent calculations and discussion.

Aryl radical covalently adsorbed on the SWNT surface. For the systems featuring covalent bonding between the aryl substituent and tube surface, the differences in geometries and orbital localization properties is much less sensitive to the long-range corrections included in the chosen DFT functional, compared to the non-covalently interacting cases (compare Figs. 1 and 2). Each calculation led to the same perpendicularly joined diazonium-SWNT dimer, as expected on account of the strong steric repulsions present at such short-ranges, despite the combination of exchange-correlation functional and basis set used. The highly localized nature of the chemical bond offsets the importance of non-dynamical correlation, compensating for inadequacies in the methodological approach that led to the discrepancies seen previously in Fig. 1. Additional structural details of these systems – as well as the computational results obtained for functionalized (8,0) and (6,5) systems – are included in Table 2. All structures show a typical sp^3 character of the C–C bond between the aryl and SWNT with a bond length of ~1.55–1.59 Å. In contrast to the electron transfer from the nanotube to the physisorbed cation, the covalent attachment of the aryl to the nanotube leads to an increase of the electronic charge density on the SWNT fragment due to a partial electron transfer from the aryl radical to SWNT via the polar bond formation.

3.2. Ground state electronic structure

Density of states (DOS) provides a simple way of tracking the simultaneous evolution of structural and electronic characteristics of two discrete chemical systems as they interact with each other. The DOS presented in Fig. 3 compares the electronic structure of non-covalent adsorption of $C_6H_5N_2^+$ onto the outer surface of the (6,2) tube with the chemically arylated version of the same (6,2) SWNT. Focusing on the functional effect on the DOS of the non-covalently and covalently functionalized SWNTs, we conclude that the electronic structures calculated with B3LYP and wB97XD models are very similar barring the greatly widened bandgap predicted by the wB97XD functional (a well known artifact of the greater fraction of orbital exchange included in its framework).

Independent of the functional used, the physisorbed aryl diazonium cation introduces additional unoccupied electronic orbitals to the energy gap of the SWNT which is seen by comparing the DOS of the pristine tube and the partial DOS of the hybrid system that was contributed by the electronic states associated with the nanotube, as presented in Fig. 3. However, the SWNT-$C_6H_5N_2^+$ complex calculated with the B3LYP model reveals very close proximity of a band of occupied states belonging to the nanotube and a band of unoccupied states belonging to the diazonium cation (see partial DOS associated with the cation in Fig. 3(a) and (b)). Such a small energy gap (the values are shown in Table 1) provides a potential explanation for the hybridization of the HOMO over the nanotube and diazonium cation we notice in Fig. 1(b) and (c), which can be explained due to the very close proximity of the HOMO level of the nanotube and the LUMO level of the diazonium cation. The DOS calculated with wB97XD model demonstrates a much wider energy gap (see Table 1). Therefore, although additional unoccupied orbitals attributed to the aryl diazonium appear inside the energy gap of the SWNT, their energies are very different from the HOMO energy of the SWNT, which hinders HOMO delocalization between the nanotube and aryl diazonium (see Fig. 1(d) and (e)).

For covalent attachment of the aryl substituent to the nanotube structure, the unoccupied orbitals of the adsorbate disappear from the energy gap, as the system rehybridizes to form a chemical bond. For all methods utilized, the energy gap of the aryl-SWNT system is lowered just slightly from the energy gap of the pristine SWNT. A small decrease in the energy gap (by 0.1–0.25 eV) marks the presence of the sp^3 defect due to the bond formation between the aryl radical and the nanotube. The polar solvent has negligible effects on the DOS of the covalently arylated SWNT. In contrast, the unoccupied orbitals of the aryl diazonium cation physisorbed on the SWNT are destabilized by the polar solvent and are up-shifted towards the edge of the conduction band of the nanotube. As a result, the energy gap of the SWNT-$C_6H_5N_2^+$ complex increases in the presence of acetonitrile, Table 1.

4. Absorption spectra

Absorption spectra calculated for the complexation of aryl diazonium cation and for the covalent annexation of the aryl substituent are presented for the (6,2) systems in Figs. 4 and 5, respectively, shown along with the spectra of the isolated tube. We also show excitation energies of the first and the most optically-active (with the largest oscillator strength) transitions for both non-covalently and covalently functionalized SWNTs in Tables 3 and 4, respectively, for all three nanotubes we considered.

Aryl diazonium cation physisorbed on SWNT the surface. Due to the formation of a charge transfer complex between the cationic absorbate and the carbon nanotube, we anticipate the SWNT-aryl diazonium system would be problematic to calculate with the B3LYP model because of the possible appearance of spurious CT excitations. Such low-lying artificial CT states with predominantly weak oscillator strengths have been observed in various systems having charge-transfer character [58,59,45,60,61]. As shown in Fig. 4, absorption spectra calculated by the B3LYP/3-21G approach has an extended low-lying energy region of transitions with very weak oscillator strengths, which is more than 1 eV red-shifted with respect to the absorption offset of the pristine nanotube (marked by the vertical arrow in Fig. 4). There are so many low-energy transitions in the case of the B3LYP-acquired spectrum that the first 20 states calculated have not reached the energy range expected for the excitations having the strongest oscillator strengths; therefore, the spectral shape of the SWNT-aryl diazonium complex obtained with the B3LYP functional drastically differs from those of the pristine SWNT. Such trends are a clear red flag for artificial CT effects.

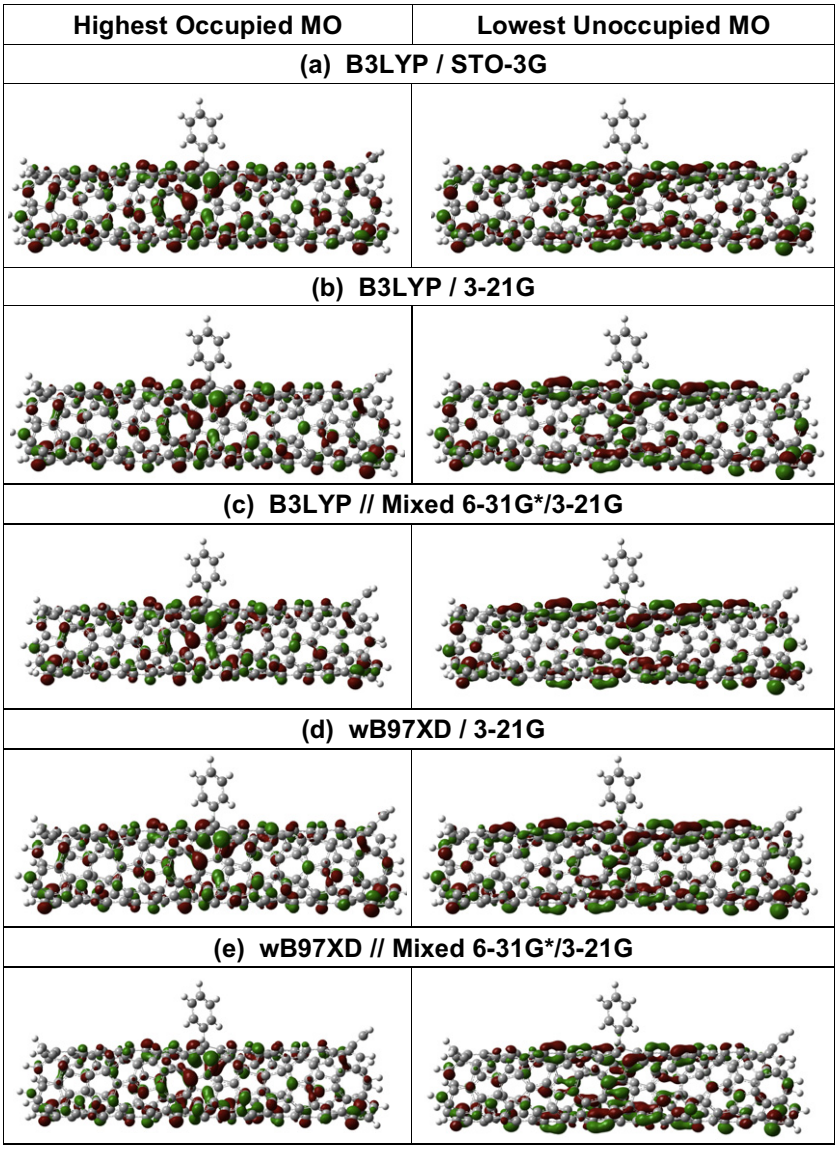

Fig. 2. Comparison of the highest-occupied (left) and lowest-unoccupied (right) molecular orbitals associated with the physisorbed C_6H_6–(6,2) systems, as calculated with different DFT methodologies. The red and green coloring of orbitals lobes depicts the alternating spatial extent of +/− phases of the electronic wavefunctions. (For interpretation of the references to colour in this figure legend, the reader is referred to the web version of this article.)

Utilization of long-range-corrected functionals (the CAM-B3LYP and wB97XD models) results in a substantial reduction of the lowest semi-dark excitation density in the absorption spectra. The strongest absorbing excitation for the $C_6H_5N_2^+$-(6,2) system occurs at 2.25 eV in the CAM-B3LYP spectrum, and at 2.35 eV in the wB97XD spectrum, which both well correlate with the brightest transition of the pristine SWNT calculated by the same functionals (see Table 3 and Fig. 4(a) and (c). These results illustrate an improvement in the quality of calculations afforded by using long-range-corrected functionals over conventional functionals, although the absolute values of optical transition energies are blue-shifted, as expected, due to the higher percentage of the HF exchange in these models.

The presence of solvent has been shown to counteract the appearance of artificial CT excitations [72,73,60] introduced to absorption spectra by semi-local exchange-correlation functionals. Our calculations in acetonitrile media prove the above concept. Incorporation of the polar media into calculations (i) reduces the number of spurious CT excitations within the B3LYP spectra, and (ii) provides very close agreement between the spectra of functionalized and pristine (6,2) nanotubes. The effect of the solvent on the absorption spectra of the pristine SWNT has insignificant effect (not shown), and has no effect on the spectra of the functionalized SWNT calculated with long-range-corrected functionals (Fig. 4(b)). Overall, when a polar solvent and/or long-range-corrected functionals are incorporated to the TD–DFT calculations, the absorption spectra of SWNTs non-covalently functionalized by the aryl diazonium cation are only slightly perturbed by the cation–SWNT interactions resulting in a small redshift ($\sim$ 50 meV) of the lowest energy bright exciton, compared to those of the pristine SWNT. Similar red shifts ($\sim$30 meV) of the absorption spectra have been experimentally found for narrow diameter SWNTs functionalized by conjugated polymers [74,75] and interpreted as a signature of π–π interactions between the SWNT and a conjugated polymer.

Aryl radical covalently adsorbed on the SWNT surface. The situation is very different for the aryl-nanotube system, as shown in Fig. 5. In contrast to the physisorption case, all three functionals provide qualitatively similar absorption spectra of the covalently

Table 2
Ground-state structural and energetic parameters for the chemisorbed C_6H_6-SWNT systems, calculated with different DFT methodologies (functional/basis set) in vacuum: the bond length between the bridging carbons on aryl substituent and on the nanotube side-wall; the angle formed between the point of attachment on the SWNT of the bonding carbon on the aryl substituent and the *para*-carbon on the aryl ring; the energy-gap of the chemically modified aryl-SWNT hybrid; the energy-gap of the pristine SWNT (for comparison); the Basis Set Superposition Error (BSSE) calculated for the complex; and, the sum of Mulliken charges only on SWNT atoms.

C_6H_6-SWNT Complex	Aryl-SWNT Bond Length [Å]	Aryl-SWNT Angle [°]	Energy gap of complex [eV]	Energy gap of pristine SWNT [eV]	BSSE [eV]	Mulliken charge on SWNT
B3LYP/STO-3G:						
(6,2)	1.589	178.078	1.89	2.00	1.44	−0.11
(6,5)	1.593	178.835	1.68	1.83	1.41	−0.12
(8,0)	1.589	178.530	1.81	2.10	1.44	−0.12
B3LYP/3-21G:						
(6,2)	1.564	178.029	1.69	1.80	0.64	−0.46
(6,5)	1.567	179.190	1.57	1.70	0.66	−0.47
(8,0)	1.566	178.661	1.75	2.02	0.64	−0.47
B3LYP/Mixed basis (3-21G and 6-31G):*						
(6,2)	1.563	177.350	1.69	1.80	0.31	−0.30
wB97XD/3-21G:						
(6,2)	1.553	177.663	4.15	4.26	0.64	−0.50
(6,5)	1.557	178.959	3.63	3.81	0.66	−0.51
(8,0)	1.555	178.179	4.00	4.52	0.64	−0.50
wB97XD/Mixed basis (3-21G and 6-31G):*						
(6,2)	1.554	176.747	4.16	4.27	0.28	−0.34

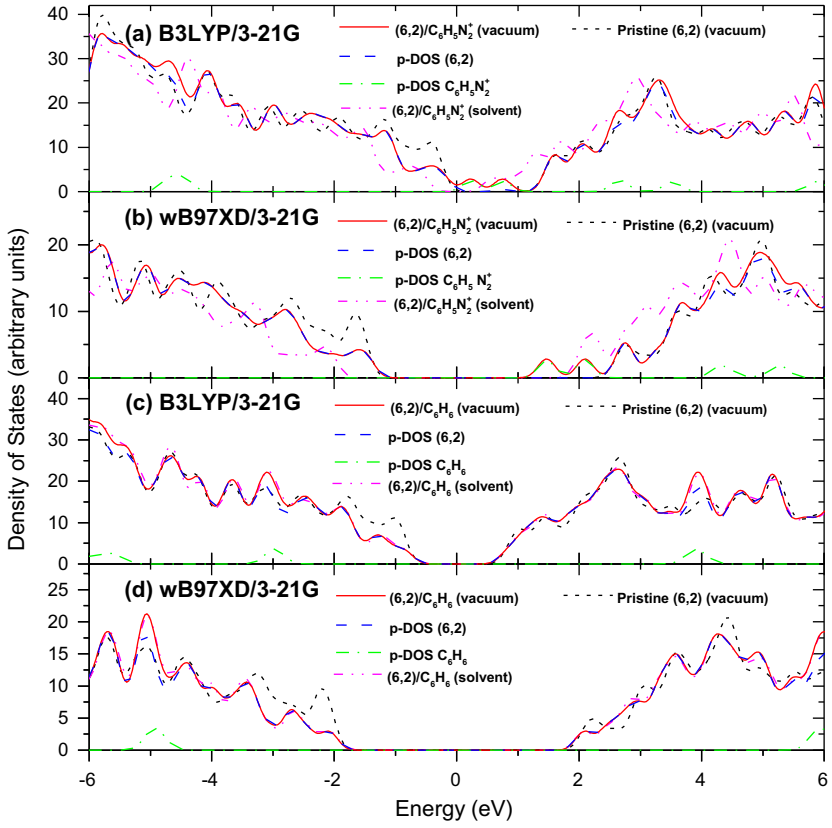

Fig. 3. Density of states (DOS) calculated for both the physisorbed (panels (a) and (b)) and chemisorbed (panels (c) and (d)) aryl diazonium derivatives on the (6,2) SWNT, as obtained at either the B3LYP/3-21G (panels (a) and (c)) or wB97XD/3-21G (panels (b) and (d)) levels of theory (with respective geometries). The red solid line corresponds the total DOS of the hybrid system in vacuum, the blue dashed line is the partial DOS (p-DOS) of the (6,2) CNT in vacuum, the green dash-dot curve represents the p-DOS of $C_6H_5N_2^+$ (panels (a) and (b)) and C_6H_6 (panels (c) and (d)), the magenta dash-dot-dot curve is the hybrid system in solvent (acetonitrile), and the black short-dashed line indicates the DOS of the pristine (6,2) nanotube in vacuum. Zero at the X-axis is chosen to be at the mid-gap of the hybrid system. DOS of the pristine nanotube was shifted, so that the first peak for the unoccupied levels coincided with those of the p-DOS of the hybrid system associated with the nanotube electronic levels. (For interpretation of the references to colour in this figure legend, the reader is referred to the web version of this article.)

functionalized aryl-SWNT system, with B3LYP calculations becoming much less conducive to artificial CT excitations. Solvation in acetonitrile has very slight effect on the absorption spectra of the arylated nanotube independent on the used functional.

Surprisingly, the covalent interaction between SWNT and functional group leads to brightening of the lowest energy exciton that is optically dark for the pristine SWNT (the lowest energy transition is marked by vertical arrows in Fig. 5), while the brightest

exciton lowers its oscillator strength. Optically forbidden (dark) and allowed (bright) excitons play an important role in influencing the photophysical behavior of SWNTs. Past investigations [76–80] suggest that the relatively low photoluminescent (PL) quantum yield of pristine SWNTs should be attributed to a dark excitonic state, positioned lower in energy than the first bright E_{11} exciton state [42,81], effectively capturing most of the exciton population. In this context, covalent functionalization of the nanotube surface might be one of many possible ways to change the selection rules governing the optical activity of SWNTs due to breaking the tube symmetry. Thus, an appearance of low-energy satellite peaks in PL spectra has been detected upon intense pulsed-laser irradiation, which creates local defects within the nanotube structure [82,83]. Analogous to the effect of the strong pulsed-laser beam, the adsorption of atomic gold [82] and hydrogen [38] onto SWNTs has been observed to cause the rising intensity of satellite peaks at the lower-energy end of the PL spectra. Red-shifted satellite peaks have also been observed in PL spectra of ozonated SWNTs [84]. Similarly, the aryl-nanotube systems we have simulated here exhibit pronounced red-shifts of the lowest state upon covalent functionalization, as well as brightening of this transition for all three nanotube systems we consider, independent on DFT functionals used for calculations (see Table 4). These transitions could be associated with the experimentally observed red-shifted satellite peaks in PL spectra [82,83,38,84].

Notably, the small size of SWNTs we consider is expected to insignificantly affect our qualitative trends observed in optical spectra of functionalized SWNTs. The effect of the nanotube size has been addressed in numerous studies [39–41]. It was shown that models of capped finite-sized SWNTs, such as those used in this study, are well suited to qualitatively reproduce the photophysics of nanotubes in the infinite length limit. Of particular relevance in this case is the length of the SWNT with respect to the size of the exciton, which is typically between ~2–3 nm [39,85], depending on the tube chirality. In our calculations, the tube length is comparable with the exciton size. Therefore, as expected, the computational absorption spectra are significantly blue shifted as compared to experimental data for these SWNTs due to confinement effects. Confinement of the tube to shorter lengths should also increase effects induced by the scattering of the exciton at the tube ends. Consequently, there is a mixing of lower energy states, leading to some gaining of oscillator strength by the nominally dark excitons (e.g., a small peak at the lower energies near the main E_{11}-peak of the pristine SWNT in Fig. 4 and Fig. 5.) Nonetheless, the qualitative picture is correct, as evidenced by our recent study [37], where we considered several longer SWNTs of 10–12 nm in length with adsorbed hydrogen atoms. Similar to

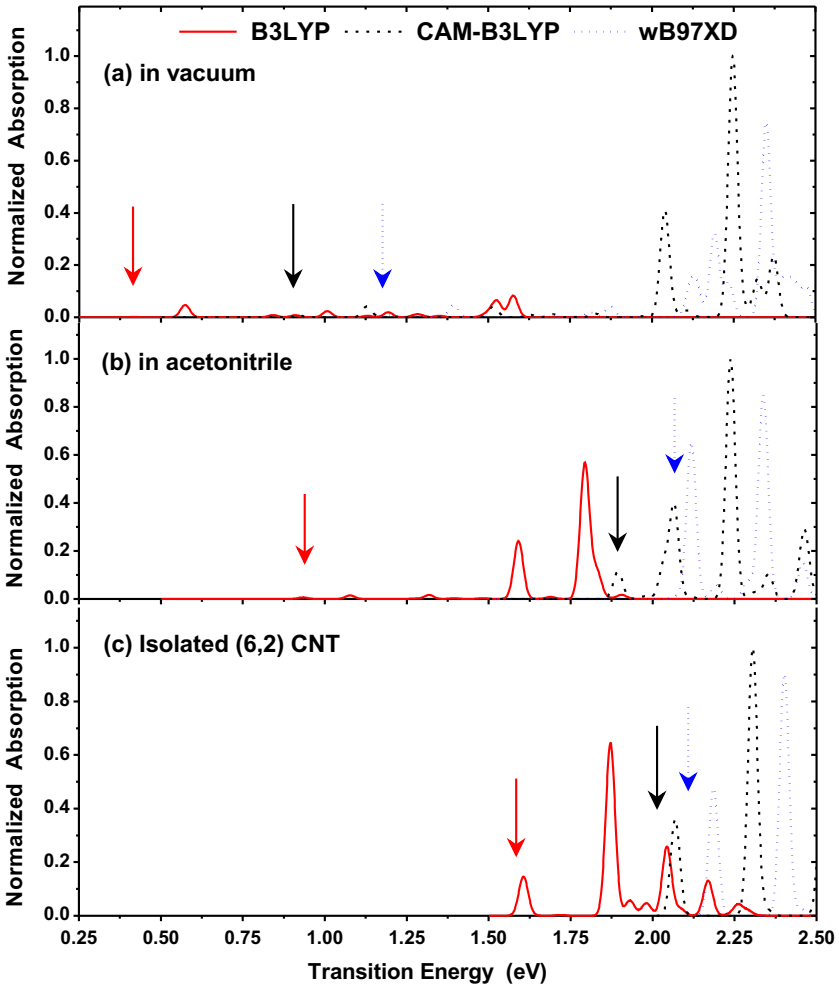

Fig. 4. Normalized absorption spectra of the physisorbed $C_6H_5N_2^+$–(6,2) complex calculated using wB97XD geometry as determined in vacuum (panel (a)) and acetonitrile solvent (panel (b)), and the absorption spectra of the pristine (6,2) nanotube (panel (c)). The red solid, blue dotted and black dashed lines correspond to the spectra calculated with the B3LYP, CAM-B3LYP and wB97XD models, respectively. (For interpretation of the references to colour in this figure legend, the reader is referred to the web version of this article.)

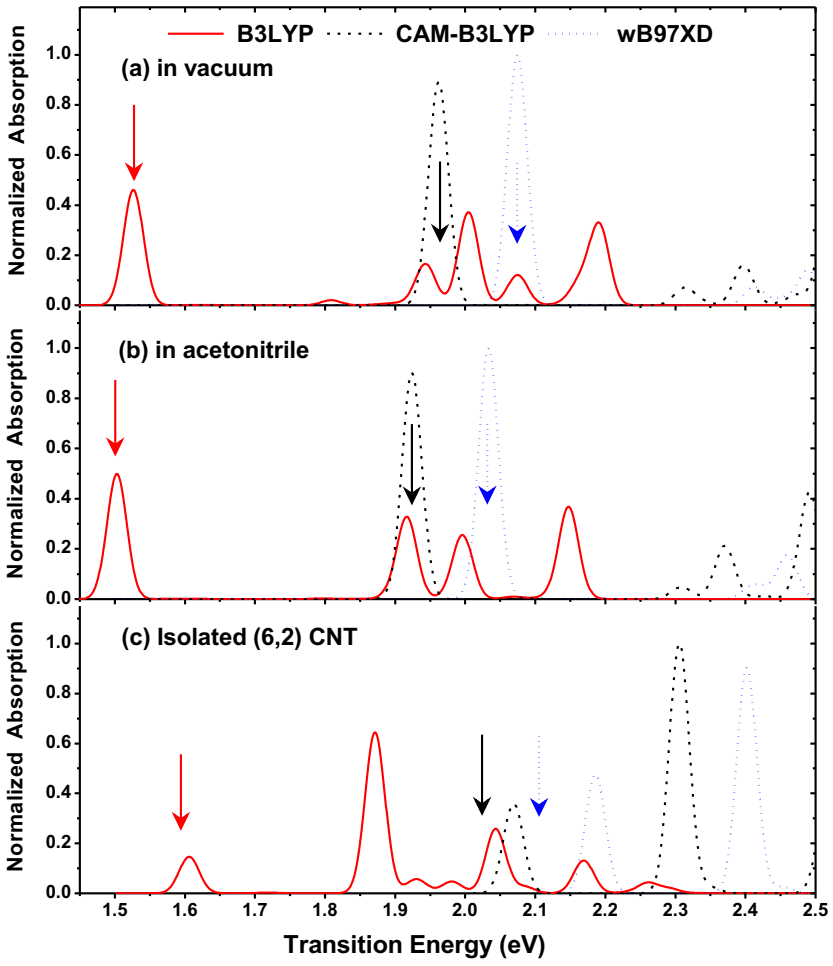

Fig. 5. Same as Fig. 4 but for the C_6H_6–(6,2) complex. Independent on the DFT methodology, covalent functionalization of the SWNT by aryl group leads to the brightening of the lowest transition (the arrow coincides with the maximum in the lowest energy absorption peak of the functionalized system, while it shifts to the red in respect to the absorption maxima in the pristine SWNT). (For interpretation of the references to colour in this figure legend, the reader is referred to the web version of this article.)

Table 3
Excited-state parameters for the physisorbed SWNT-$C_6H_5N_2^+$ systems, calculated with different TD–DFT methodologies (functional/basis set): The energy of the very first transition – absorption onset – calculated for the complexed system in vacuum and in acetonitrile solvent and the energy of the most optically-active transition calculated in vacuum and in acetonitrile solvent. The oscillator strength, *f*, of each transition is shown in parenthesis.

$C_6H_5N_2^+$/SWNT	Vaccum		Solvent	
	Abs. Onset eV (*f*)	Max. Abs. eV (*f*)	Abs. Onset eV (*f*)	Max. Abs. eV (*f*)
TD-B3LYP/3-21G:				
(6,2)	0.42 (0.002)	1.58 (0.129)	0.93 (0.016)	1.79 (1.360)
(6,5)	0.24 (0.021)	0.39 (0.073)	0.89 (0.026)	1.54 (2.222)
(8,0)	0.16 (0.000)	0.59 (0.020)	0.91 (0.004)	1.86 (0.112)
TD-CAM-B3LYP/3-21G:				
(6,2)	0.92 (0.010)	2.25 (1.551)	1.89 (0.273)	2.24 (2.408)
(6,5)	0.73 (0.021)	1.93 (3.259)	1.77 (0.000)	1.91 (4.486)
(8,0)	0.66 (0.007)	2.12 (0.100)	1.98 (0.043)	2.29 (0.225)
TD-wB97XD/3-21G:				
(6,2)	1.20 (0.015)	2.35 (1.160)	2.07 (0.031)	2.34 (1.585)
(6,5)	1.04 (0.026)	2.02 (3.747)	1.84 (0.000)	1.99 (4.220)
(8,0)	0.95 (0.009)	2.37 (0.138)	2.13 (0.002)	2.89 (0.314)

findings presented in Fig. 5, hydrogenation of the nanotube surface leads to a red-shift and brightening of the lowest excitonic state [37]. Therefore, we expect modeling based on short functionalized SWNTs provides qualitatively reasonable results.

However, experimental results on SWNTs functionalized by diazonium derivatives with nitro- and chloro-groups on the aryl ring has shown a blue shift, a weakening of intensities, and significant broadening of the absorption spectrum of SWNTs upon functionalization [86]. In our calculations, E_{11} band also experiences a very slight blue shift, broadening, and decrease in intensity due to covalent-interaction between the aryl adsorbate and SWNT (see Fig. 5). However, these blue-shifts are tiny and do not compensate a new bright state at the red range of the spectra appeared upon functionalization. On the other hand, our previous simulations of SWNTs

Table 4
Excited-state parameters for the chemisorbed C_6H_6-SWNT systems, compared to the isolated pristine SWNT, calculated with different TD–DFT methodologies (functional/basis set) in vacuum and in acetonitrile solvent: The energy of the very first transition – absorption onset – of the complexed system, the energy of the most optically-active transition of the complex, and the energy of bright E_{11} exciton of the pristine SWNT. The oscillator strength, *f*, of each transition is shown in parenthesis.

C_6H_6-SWNT	Vaccum			Solvent		
	Abs. Onset of complex eV (f)	Max. Abs. of complex eV (f)	E_{11} SWNT eV (f)	Abs. Onset of complex eV (f)	Max. Abs. of complex eV (f)	E_{11} SWNT eV (f)
B3LYP/3-21G:						
(6,2)	1.53 (0.667)	1.53 (0.667)	1.87 (1.319)	1.50 (1.097)	1.50 (1.097)	1.82 (1.802)
(6,5)	1.37 (0.771)	1.67 (0.894)	1.60 (2.373)	1.35 (1.309)	1.35 (1.309)	1.55 (3.549)
(8,0)	1.48 (0.061)	1.49 (0.115)	1.84 (0.059)	1.48 (0.225)	1.48 (0.225)	1.84 (0.099)
CAM-B3LYP/3-21G:						
(6,2)	1.96 (1.291)	1.96 (1.291)	2.30 (2.046)	1.92 (1.983)	1.92 (1.983)	2.26 (1.593)
(6,5)	1.74 (1.588)	2.09 (1.605)	1.98 (3.798)	1.71 (2.445)	1.71 (2.445)	1.93 (5.030)
(8,0)	1.81 (0.145)	2.85 (0.412)	2.15 (0.154)	1.80 (0.435)	2.83 (0.852)	2.15 (0.238)
wB97XD/3-21G:						
(6,2)	2.07 (1.447)	2.07 (1.447)	2.40 (1.848)	2.03 (2.199)	2.03 (2.199)	2.36 (2.149)
(6,5)	1.83 (1.875)	1.83 (1.875)	2.06 (3.219)	1.80 (2.807)	1.80 (2.807)	1.93 (5.030)
(8,0)	1.86 (0.186)	2.95 (0.388)	2.22 (0.194)	1.85 (0.478)	2.93 (1.006)	2.22 (0.301)

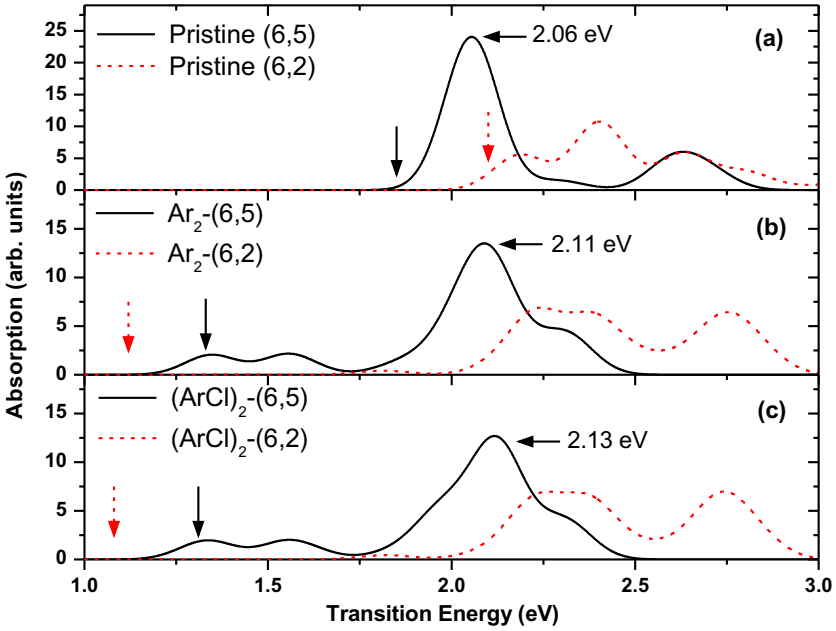

Fig. 6. Absorption spectra of (6,5) and (6,2) SWNTs and their functionalized derivatives calculated in vacuum using wB97XD/3-21G* methodology. (a) Absorption spectra of pristine tubes; (b) Doubly arylated-SWNT hybrids; (c) chlorinated derivatives of the doubly arylated systems. Functionalization is realized via circumferential attachment of molecules to the different carbon rings at the opposite sides of the nanotube. Vertical arrows define the lowest-energy transition with the black color corresponding to the (6,5) and red to the (6,2) SWNT. (For interpretation of the references to colour in this figure legend, the reader is referred to the web version of this article.)

with attached hydrogen in different positions [37] have demonstrated that the energy and the oscillator strength of the lowest-energy transitions are very sensitive to the position of the defect. Some attachments lead to very delocalized orbitals originated from the chemical defect. In this case, the brightening of the lowest exciton is observed, similar to our results shown in Fig. 5. Other attachments, in particular, when two hydrogens are significantly distanced from each other being attached to different carbon rings of the SWNT surface, result on strong localization of transition orbitals on the sp^3 defects, which lead to optically forbidden trap states.

To investigate the effect of the aryl position at the SWNT surface on the optical spectra, as well as the effect of the substituents on the aryl group, we have performed calculations of the doubly arylated (6,2) and (6,5) SWNTs and their chlorinated derivatives attached to the different SWNTs rings at the opposite sides of the tube. The absorption spectra of these systems are presented in Fig. 6. Of the two chiral types studied, the noticeable blue-shift of the E_{11} band was only apparent for the (6,5) nanotube upon aryl and chlorobenzene attachment. In fact, circumferential attachment of the aryl rings results in a 50 meV blue shift of this peak, and of chlorobenzene moiety leads to a stronger 70 meV blue shift, relative to the pristine (6,5) nanotube. This is consistent with the experimentally observed blue-shifts [86]. On a side note, the low lying semi-bright peaks below the E_{11} peak appear for the (6,5) SWNT, while for the (6,2) SWNT, the lowest-energy states are nearly dark. The enhanced oscillator strength of this transition in (6,5) SWNT might be artificially increased due to the short size of the SWNT.

Overall, E_{11} peak in the absorption spectra of functionalized SWNTs exhibits a small blue shift and broadening upon aryl and chlorobenzene attachments, which are enhanced when the dipole moment of the functional group increases. These trends, however, are sensitive to the tube chirality and the position of the chemical

defect on the nanotube surface. Similarly, the energy and oscillator strength of the very lowest exciton also depend on the alignment of the covalently-attached molecule with respect to the nanotube surface. At some positions, in particular, when both defects are located at the same carbon-ring of the nanotube, there is a marked increase in the oscillator strength, suggesting that the PL efficiency of semiconducting SWNTs may be controlled through selective chemical functionalization. It is important to note, however, that when an ion instead of the neutral group is covalently attached to the SWNT, many additional lower-energy defect-localized states with zero transition dipole moments are appeared. In this case, the PL is expected to be quenched. Because the SWNT-diazonium reaction occurs in the presence of ions with a high probability that charged species might be covalently interact with the nanotube, PL quenching is expected instead of enhancement.

5. Conclusions

The strong correlations between the structure and electronic/optical properties of SWNTs functionalized covalently or non-covalently with aryl diazonium salts, emphasize that molecular geometry controls the spatial distribution of charge density. Our calculations show that modern long-range corrected functionals greatly improve description of the non-covalent complexation by the aryl diazonium cation, partially mending the incomplete treatment of van der Waals and London interactions handicapping many older DFT functionals. Significant π–π overlap between the diazonium complex and the nanotube is realized by the parallel geometry and molecule-nanotube distances of $\sim$3.2 Åas calculated at the wB97XD/3-21G level of theory. In contrast, B3LYP calculations predict incorrect binding of the aryl diazonium cation to the SWNT wall, which could be rectified via incorporating basis sets larger than 3-21G and adding the CP corrections to the computational methodology. Improved band structures are also seen in the electronic density of states calculated using the wB97XD functional, resulting in a lesser degree of hybridization among electronic states, as expected for the physisorbed molecules.

We found that upon physisorption, a small portion of electronic charge density is transferred from the nanotube to the aryl diazonium cation. This indicates, that despite an absence of direct chemical bonding, the cation is stabilized through formation of the charge-transfer SWNT-aryl diazonium complex, which agree with the suggested reaction's scenario from experimental investigations [21–23]. However, the degree of the electron transfer from the nanotube to the molecule is very sensitive to the polar solvent, which can dramatically screen out the charge transfer. Thus, our calculations confirm the important role that the solvent environment plays during the reaction between SWNT and aryl diazonium, as has been experimentally revealed for these systems in the presence of different surfactants [26,27].

Calculations of excited states show dramatic divergences of the absorption onsets in the simulated spectra of non-covalently functionalized SWNTs using different DFT models. This exemplifies the importance of the methodology choice for TD–DFT studies of optical properties. TD-B3LYP/3-21G calculations produce many artificial low-energy semi-dark charge transfer states in the absorption spectra of SWNT-aryl diazonium complexes. In contrast, the CAM-B3LYP and wB97XD functionals lead to a drastic reduction of these spurious CT states. Incorporation of polar solvent model also reduces the number of CT transitions obtained with the B3LYP/3-21G technique, while it has an insignificant effect on the absorption spectra of pristine SWNTs and non-covalently functionalized SWNTS calculated with range-corrected functionals. These results suggest extending caution for DFT and TD–DFT calculations of such highly conjugated and charged systems interacting via weak electrostatic forces and π–π stacking, as popular DFT models may produce erroneous results.

Considering only the cases where long-range-corrected functionals were used, we found that the absorption spectra of SWNTs non-covalently functionalized by the aryl diazonium cation are only slightly perturbed by the cation–SWNT interactions resulting in a small redshift of the lowest energy bright exciton, compared to those of the pristine SWNT. Such red-shifts are attributed to π–π interactions between the SWNT and the molecule. In contrast, our calculations of covalently bound complexes demonstrate significant red-shift and a brightening of the lowest exciton (that is optically dark in pristine SWNTs) due to formation of the local chemical defect originating from the aryl–SWNT covalent interaction. However, the energy and oscillator strength of the very lowest exciton strongly depend on the alignment of the covalently-attached molecule with respect to the nanotube surface, as well as on the nanotube chirality. At some positions, in particular, when both defects are located at the same carbon-ring of the nanotube, the lowest exciton becomes optically bright; thus predicting that the PL efficiency of semiconducting SWNTs may be controlled through selective chemical functionalization. Appearance of the lowest-energy optically allowed excitonic state is accompanied by decrease in intensity of E_{11}. Overall, the E_{11} band experiences blue-shifts (of $\sim$50–70 meV), broadening and intensity weakening upon covalent attachments of aryl and its chlorinated derivatives to the different carbon-rings of the SWNT, which are enhanced when the dipole moment of the functional group increases. This trend also is sensitive to the tube chirality and the position of the chemical defect on the nanotube surface.

Acknowledgements

S.T. and J. R. acknowledge support of the US Department of Energy and Los Alamos National Laboratory (LANL) Directed Research and Development funds. S.K. and M.L.M. acknowledge NDSU Advance FORWARD program sponsored by NSF HRD-0811239 and ND EPSCoR through NSF grant no. EPS-0814442. Authors thank Dr. Ekaterina Badaeva for fruitful discussions. We acknowledge support of Center for Integrated Nanotechnology (CINT) and Center for Nonlinear Studies (CNLS). Los Alamos National Laboratory is operated by Los Alamos National Security, LLC, for the National Nuclear Security Administration of the U.S. Department of Energy under contract DE-AC52-06NA25396.

References

[1] S. Iijima, T. Ichihashi, Nature 363 (1993) 603.
[2] C. Staii, A.T. Johnson, Nano Lett. 5 (2005) 1774.
[3] J. Kong, N.R. Franklin, C. Zhou, M.G. Chapline, S. Peng, K. Cho, H. Dai, Science 287 (2000) 622.
[4] L. An, Q. Fu, C. Lu, J.J. Liu, Am. Chem. Soc. 126 (2004) 10520.
[5] C.J. Wang, Q. Cao, T. Ozel, A. Gaur, J.A. Rogers, M.J. Shim, Am. Chem. Soc. 127 (2005) 11460.
[6] M. Dresselhaus, G. Dresselhaus, P. Avouris (Eds.), Carbon Nanotubes: Synthesis, Structure, Properties and Applications, Springer Series: Topics in Applied Physics, 80, Springer-Verlag, Berlin, Germany, 1996.
[7] C. Charlier, X. Blase, S. Roche, Rev. Mod. Phys. 79 (2007) 677.
[8] Y.C. Chen, N.R. Raravikar, L.S. Schadler, P.M. Ajayan, Y.P. Zhao, T.M. Lu, G.C. Wang, X.C. Zhang, Appl. Phys. Lett. 81 (2002) 975.
[9] S.Y. Set, H. Yaguchi, Y. Tanaka, M.J. Jablonski, Lightwave Technol. 22 (2004) 51.
[10] L.M. Ericson, P.E.J. Pehrsson, Phys. Chem. B 109 (2005) 20276.
[11] M.J. O'Connell, E.E. Eibergen, S.K. Doorn, Nat. Mater. 4 (2005) 412.
[12] M. Kanungo, H. Lu, G.G. Malliaras, G.B. Blanchet, Science 323 (2009) 234–237.
[13] X. Pan, L.L. Li, M. Chan-Park, Small 6 (2010) 1311–1320.
[14] M. Zheng, A. Jagota, E.D. Semke, B.A. Diner, R.S. Mclean, S.R. Lustig, R.E. Richardson, N.G. Tassi, Nat. Mater. 2 (2003) 338.
[15] D.A. Yarotski, S. Kilina, A.A. Talin, S. Tretiak, O.V. Prezhdo, A.V. Balatsky, A.J. Taylor, Nano Lett. 9 (2009) 12.
[16] X. Tu, S. Manohar, A. Jagota, M. Zheng, Nature 460 (2009) 250–253.
[17] F.F. Gadallah, R.M.J. Elofson, Org. Chem. 34 (1969) 3335.
[18] J.L. Bahr, J. Yang, D.V. Kosynkin, M.J. Bronikowski, R.E. Smalley, J.M.J. Tour, Am. Chem. Soc. 123 (2001) 6536.

[19] W. Kim, M.L. Usrey, M.S. Strano, Chem. Mater. 19 (2007) 1571.
[20] N. Nair, W. Kim, M.L. Usrey, M.S.J. Strano, Am. Chem. Soc. 129 (2007) 3946.
[21] M.L. Usrey, E.S. Lippmann, M.S.J. Strano, Am. Chem. Soc. 127 (2005) 16129.
[22] M.S.J. Strano, Am. Chem. Soc. 125 (2003) 16148.
[23] M.S. Strano, C.A. Dyke, M.L. Usrey, P.W. Barone, M.J. Allen, H.W. Shan, C. Kittrell, R.H. Hauge, J.M. Tour, R.E. Smalley, Science 301 (2003) 1519.
[24] C.D. Doyle, J.R. Rocha, R.B. Weisman, J.M.J. Tour, Am. Chem. Soc. 130 (2008) 6795.
[25] G. Schmidt, S. Gallon, S. Esnouf, J.P. Bourgoin, P. Chenevier, Chem. A Eur. J. 15 (2009) 2101–2110.
[26] A.J. Blanch, C.E. Lenehan, J.S.J. Quinton, Phys. Chem. C 116 (2012) 1709.
[27] A.J. Hilmer, T.P. McNicholas, S. Lin, J. Zhang, Q.H. Wang, J.D. Mendenhall, C. Song, D.A. Heller, P.W. Barone, D. Blankschtein, M.S. Strano, Langmuir 28 (2012) 1309.
[28] B.G. Sumpter, D. Jiang, V. Meunier, Small 4 (2008) 2035.
[29] H. Wang, J. Xu, Chem. Phys. Lett. 477 (2009) 176.
[30] S. Lin, A.J. Hilmer, J.D. Mendenhall, M.S. Strano, D. Blankschtein, J. Am. Chem. Soc. 134 (2012) 8194.
[31] J. Wang, H. Chu, Y. Li, ACS Nano 2 (2008) 2540–2546.
[32] T. Nongnual, S. Nokbin, P. Khongpracha, P.A. Bopp, J. Limtrakul, Carbon 48 (2010) 1524.
[33] S. Grimme, WIREs Comput. Mol. Sci. 1 (2011) 211–228.
[34] R.G. Parr, W. Yang, Density-Functional Theory of Atoms and Molecules, Oxford University Press, New York, 1989.
[35] J. Chai, M. Head-Gordon, Phys. Chem. Chem. Phys. 10 (2008) 6615.
[36] T. Yanai, D.P. Tew, N.C. Handy, Chem. Phys. Lett. 393 (2004) 51.
[37] S. Kilina, J. Ramirez, S. Tretiak, Nano Lett. 12 (2012) 2306.
[38] K. Nagatsu, S. Chiashi, S. Konabe, Y. Homma, Phys. Rev. Lett. 105 (2010) 157403.
[39] S. Kilina, S. Tretiak, Adv. Funct. Mater. 17 (2007) 3405.
[40] P.T. Araujo, S.K. Doorn, S. Kilina, S. Tretiak, E. Einarsson, S. Maruyama, H. Chacham, M.A. Pimenta, A. Jorio, Phys. Rev. Lett. 98 (2007) 067401.
[41] A.P. Shreve, E.H. Haroz, S.M. Bachilo, R.B. Weisman, S. Tretiak, S. Kilna, S.K. Doorn, Phys. Rev. Lett. 98 (3) (2007) 037405.
[42] S. Kilina, E. Badaeva, A. Piryatinski, S. Tretiak, S. Saxena, A.R. Bishop, Phys. Chem. Chem. Phys. 11 (2009) 4113.
[43] A.D.J. Becke, Chem. Phys. 98 (1993) 5648.
[44] P.J. Stephens, F.J. Devlin, C.F. Chabalowski, M.J.J. Frisch, Phys. Chem. 98 (1994) 11623.
[45] A. Dreuw, M. Head-Gordon, Chem. Rev. 105 (2005) 4009.
[46] J.F. Dobson, K. McLennan, A. Rubio, J. Wang, T. Gould, H.M. Le, B.P. Dinte, Aust. J. Chem. 54 (2001) 513.
[47] S. Kristyan, P. Pulay, Chem. Phys. Lett. 229 (1994) 175.
[48] J.C. Slater, Phys. Rev. 36 (1930) 57.
[49] J.S. Binkley, J.A. Pople, W.J.J. Hehre, Am. Chem. Soc. 102 (1980) 939.
[50] Gaussian 09, revision a.01. et al. M.J.F.
[51] V. Barone, M. Cossi, J.J. Tomasi, Comput. Chem. 19 (1998) 404–417.
[52] M. Cossi, N. Rega, G. Scalmani, V.J. Barone, Comput. Chem. 24 (2003) 669–681.
[53] S. Tretiak, K. Igumenshchev, V. Chernyak, Phys. Rev. B 71 (2005) 33201.
[54] K.I. Igumenshchev, S. Tretiak, V.Y.J. Chernyak, Chem. Phys. 127 (11) (2007) 1–10.
[55] C. Katan, S. Tretiak, M.H.V. Werts, A.J. Bain, R.J. Marsh, N. Leonczek, N. Nicolaou, E. Badaeva, O. Mongin, M.J. Blanchard-Desce, Phys. Chem. B 111 (32) (2007) 9468–9483.
[56] S. Tretiak, Nano. Lett. 7 (2007) 2201.
[57] G.D. Scholes, S. Tretiak, T.J. McDonald, W.K. Metzger, C. Engtrakul, G. Rumbles, M.J.J. Heben, Phys. Chem. C 111 (30) (2007) 11139–11149.
[58] A. Dreuw, J.L. Weisman, M.J. Head-Gordon, Chem. Phys. 119 (2003) 2943.
[59] A. Dreuw, M.J. Head-Gordon, Am. Chem. Soc. 126 (2004) 4007.
[60] E. Badaeva, V.V. Albert, S. Kilina, A. Koposov, M. Sykora, S. Tretiak, Phys. Chem. Chem. Phys. 12 (2010) 8902–8913.
[61] R.J. Magyar, S.J. Tretiak, Chem. Theory Comput. 3 (2007) 976.
[62] H. Park, J. Zhao, J.P. Lu, Nanotechnology 16 (2005) 635.
[63] J.J. Zhao, H.K. Park, J. Han, J.P.J. Lu, Phys. Chem. B 108 (2004) 4227.
[64] C.J. Cramer, Essentials of Computational Chemistry, 2nd ed., Wiley-VCH: West Sussex, 2004.
[65] W. Koch, M.A. Holthausen, Chemists Guide to Density Functional Theory, 2nd ed., Wiley-VCH: Verlag, 2001.
[66] V.V. Albert, S.A. Ivanov, S. Tretiak, S.V.J. Kilina, Phys. Chem. C 115 (2011) 15793–15800.
[67] S.F. Boys, F. Bernard, Mol. Phys. 19 (1970) 553.
[68] M.O. Sinnokrot, E.F. Valeev, C.D.J. Sherrill, Am. Chem. Soc. 124 (2002) 10887–10893.
[69] H. Zollinger, Angewandte Chemie 17 (1978) 141.
[70] J.C. Scaiano, N. Kim-Thuan, Can. J. Chem. 60 (1982) 2286.
[71] B.F. Minaev, S.V. Bondarchuk, Russ. J. Appl. Chem. 82 (2009) 840.
[72] M.A. Aguilar, F.J. Olivares del Valle, J.J. Tomasi, Chem. Phys. 98 (1993) 7375.
[73] M. Cossi, V.J. Barone, Phys. Chem. A 104 (2000) 10614.
[74] L. Lüer, S. Hoseinkhani, M. Meneghetti, G. Lanzani, Phys. Rev. B 81 (15) (2010) 155411.
[75] Y.K. Kang, O.L. Lee, S.H. Deria, T.H. Kim, D.A. Park, J.G. Bonnell, M.J. Saven Therien, Nano Lett. 9 (4) (2009) 1414–1418.
[76] V. Perebeinos, J. Tersoff, P. Avouris, Nano. Lett. 5 (2005) 2495.
[77] H.B. Zhao, S. Mazumdar, Phys. Rev. Lett. 93 (2004) 157402.
[78] C.D. Spataru, S. Ismail-Beigi, R.B. Capaz, S.G. Louie, Phys. Rev. Lett. 95 (2005) 247402.
[79] R.B. Capaz, C.D. Spataru, S. Ismail-Beigi, S.G. Louie, Phys. Rev. B 74 (2006) 121401.
[80] H. Zhao, S. Mazumdar, C.X. Sheng, M. Tong, Z.V. Vardeny, Phys. Rev. B 73 (2006) 75403.
[81] S. Kilina, S. Tretiak, S.K. Doorn, Z. Luo, F. Papadimitrakopoulos, A. Piryatinski, A. Saxena, A.R. Bishop, Proc. Nat. Acad. Sci. USA 105 (2008) 6797–6802.
[82] H. Harutyunyan, T. Gokus, A.A. Green, M.C. Hersam, M. Allegrini, A. Hartschuh, Nano Lett. 9 (2009) 2010–2014.
[83] R. Matsunaga, K. Matsuda, Y. Kanemitsu, Phys. Rev. B 81 (2010) 033401.
[84] S. Ghosh, S.M. Bachilo, R.A. Simonette, K.M. Beckingham, R.B. Weisman, Science 330 (2010) 1656–1659.
[85] L. Luer, S. Hoseinkhani, D. Polli, J. Crochet, T. Hertel, G. Lanzani, Nature Phys. 5 (2009) 54–58.
[86] C. Fantini, M.L. Usrey, M.S.J. Strano, Phys. Chem. C 111 (48) (2007) 17941–17946.